Finite Element Modeling of Crack initiation and Crack Growth

S.Shamasundar, Biradar Laxman S., Chidanada G, Sachin B. M.

ProSIM R & D Center
21/B, 9th Main, ShankaraNagara, Mahalakshmi Puram, Bangalore 560096
Tel/fax: +91 8023578292 email: info@pro-sim.com, URL: www.pro-sim.com

Abstract

In the remaining life assessment and life extension strategies for ageing aircrafts, a scientific study of the crack initiation and crack growth are important factors. The latest developments in the science of fracture mechanics can be used to study the extent of degradation of the component (or system) and assess the remaining cycle time before the crack grows to critical size to cause failure.

Finite element modeling is used to analyse the crack growth and predict the cycles to failure. This forms an important feature of the life assessment and extension strategies. Often for the old fleet of imported air crafts, the design data and the material data are not available. Generation of the 3D CAD models by reverse engineering and thereby the generating the design data is an important step in this activity. Similarly, an assessment of the basic material properties of the nascent material (flow properties, thermal properties, fracture and fatigue properties, creep properties etc.) is important. The extent of degradation of the component / system during service also has to be assessed. These issues form the basic input criteria for assessment of the damage and life extension methodology.

ProSIM is a R&D group working in the area of Remaining Life Assessment and life extension by using state of the art finite element (and other) computer simulation techniques. The basic concepts of fatigue are explained in this paper. Application of FEM to crack propagation is explained by selected case studies.

Keywords: Crack growth / propagation, modeling, fatigue, crack propagation, stress intensity factor, finite element, remaining life assessment, life extension.

1. Introduction

Fracture mechanics is the science of predicting the behaviour of material in the presence of flaws or cracks. Such flaws may be the result, for example, of manufacturing processes or they may initiate over time as the result of in-service loading. The cracks may propagate as a result of time dependent load effects or due to cyclic loading.

In complex 3D geometries, geometric discontinuities such as chamfers / stiffeners are potential zones for crack initiation. Further complications may be introduced from variety of sources including residual stress effects, propagation along interface of dissimilar metals, non-homogeneity of metals or large grained or anisotropic materials.

Structures designed only from static load considerations may not reach design life because of the effect of crack propagation due to dynamic loading. This is a major issue in a variety of industries in which damage tolerance is a key part of the design process. In aerospace structures, gas turbine engines, pressure vessels and pipelines failure could lead to catastrophic failure and loss of life. The conventional design using empirical methods is conservative, and use sub-optimal solutions. Thus, there is an increasing demand for reliability and performance based design. During service, safety assessment and certification procedures call for the prediction of future crack growth rates in service.

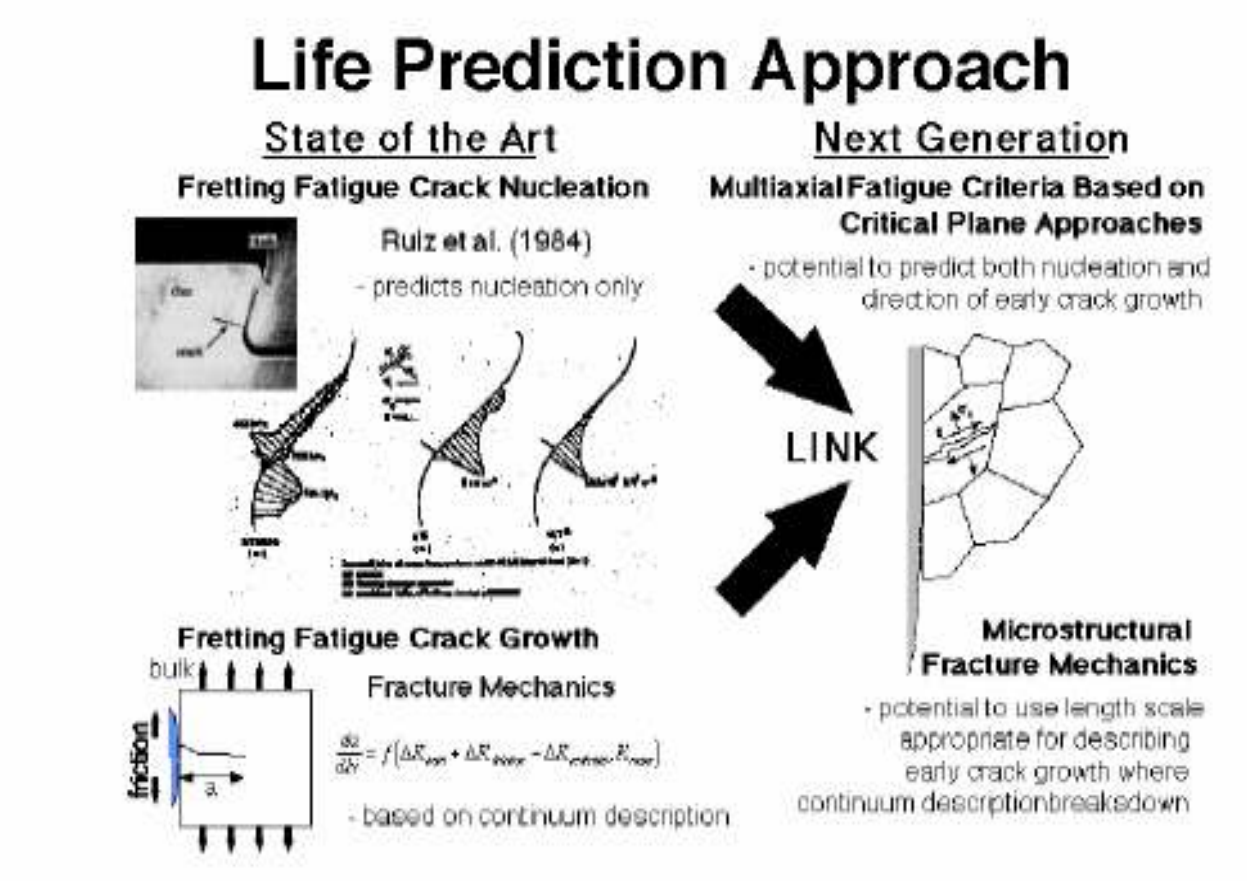

Figure1. Life prediction approach

The financial costs associated with the reduction of service intervals (TBO) or between repair and replacement of components /systems is a crucial factor. There are several reports in literature modeling methodologies that can be used predicting fretting fatigue, nucleation and crack growth. Figure 1 shows the directions for next generation in modeling[1]. Fretting fatigue occurs when two bodies are in contact and undergo a small oscillatory slip and at least one of the bodies is subjected to cyclic loading. It is often the root cause of fatigue crack nucleation. Nucleation involves all the processes leading to

the formation of a crack typically of the order of 10 μm. The crack growth (figure 1) occurs due to additional crack driving forces under fatigue. It is an empirical model that has been shown to accurately predict the location of fretting fatigue cracks along the contact interfaces. Next generation nucleation models may be based on multiaxial fatigue criteria, such as critical plane approach, which can predict the nucleation location as well as the direction of early crack growth.

Fatigue failure is the phenomenon leading to fracture under repeated or fluctuating stresses that are less than the tensile strength of the material. There are three stages of fatigue failure: initiation, propagation, and final fracture. Figure 2 shows the three phases of the crack formation and failure.

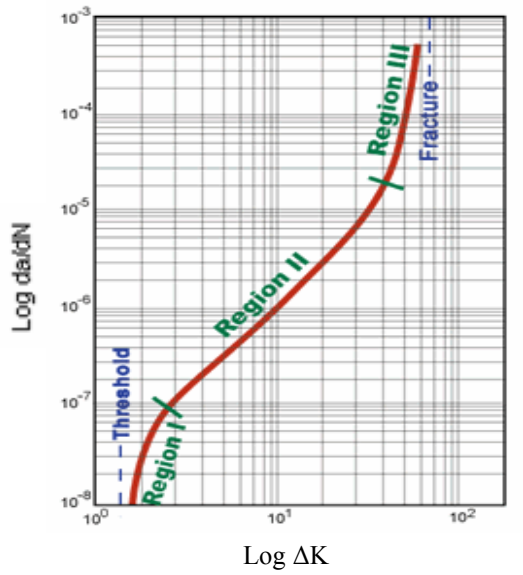

Figure 2 Typical da/dN curve.

The initiation site is minute, never extending for more than two to five grains around the origin. The crack initiation occurs at locations of high stress concentrations. The crack initiation site is always parallel to the shear stress direction. As repetitive loading continues, the direction of the crack changes perpendicular to the tensile stress direction. It should be noted that ductile fracture is caused by shear stress components, whereas brittle fracture is caused by tensile stress components. At the tip of the crack, localized extremely sharp stress concentration zones are created. Cyclic loading tends to drive the crack deeper into the metal. With each cycle the depth of the crack advances by one "striation". Striations are very tiny, closely spaced ridges that identify the tip of the crack at some point in time. Although striations are the most characteristic microscopic evidence of fatigue fracture, they are not always present on fatigue fracture surfaces.

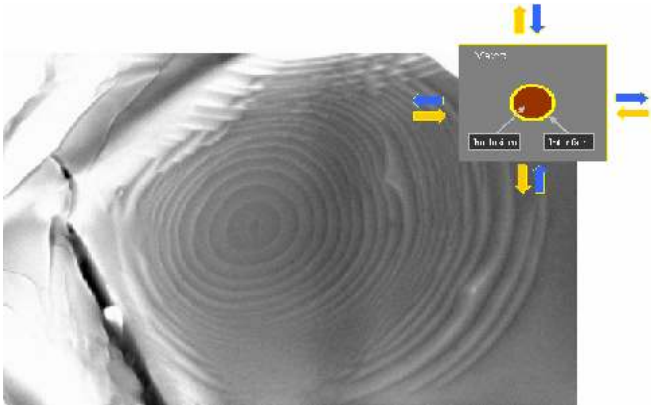

Figure 3. Fatigue separation of particulate in 2014-T6511[2]

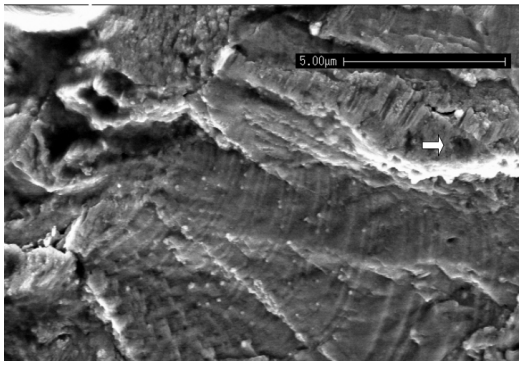

Figure 4 Notch root crack – near-threshold, high local stress[2]

The mere presence of a crack does not condemn a component or structure to be unsafe and hence unreliable. It is important to determine under cyclic loading, the number of cycles when the crack size reaches critical length to cause failure. By knowing how a crack propagates and its rate of propagation, one should be able to estimate the residual service life of a component under normal service loading conditions. Crack propagation enables one to predict the period of sub-critical crack growth and hence service life of a component.

The crack propagation analysis includes in the following area:

1. Crack growth and cycles to fail prediction.
2. Studying the effects of a surface treatment such as shot peening, laser shock peening etc. to improve the life of component.
3. Studying the effectiveness of crack repair systems, remedial work, modifications or design changes.
4. Establishing inspection and maintenance regimes.

2. Requirements of crack growth analysis

Crack propagation analysis is based on calculation of fracture mechanics parameters such as the stress intensity factor, J-integral, and energy release rate G. These parameters determine the local effect of the crack on the structure.

After the calculation of fracture mechanics parameters for a particular crack in a structure under a given load, the next task is to convert that information into crack growth. This requires the knowledge load history and the appropriate material crack growth data. Crack growth is calculated over a number of load cycles or an elapsed time respectively. The method used to determine the crack growth depends upon the numerical technique implemented in the analysis. For a closed form method in which fracture parameters can be quickly and cheaply re-calculated, cycle-by-cycle integration is possible. In addition the analysis should be able to consider the effects such as residual stress and load interactions, creep and fatigue interactions.

3. Fracture mechanics

The primary fracture mechanics parameters which are important in crack propagation are:

1. Stress intensity factor, K
2. J – integral
3. Energy release rate, G

The stress intensity factor approach was developed by Irwin in the 1950s. He extended Griffith's work on brittle fracture to ductile materials. He developed the concept of strain energy release rate. Irwin's work led to the foundations for the concept of linear elastic fracture mechanics (LFEM) which is still fundamental concept in most of the crack propagation analysis.

For linear elastic analysis the concepts of energy release rate and stress intensity factors are closely related. The stress intensity factors describe the magnitude of elastic stress field at the crack front. The basic three modes of fracture are as shown below.

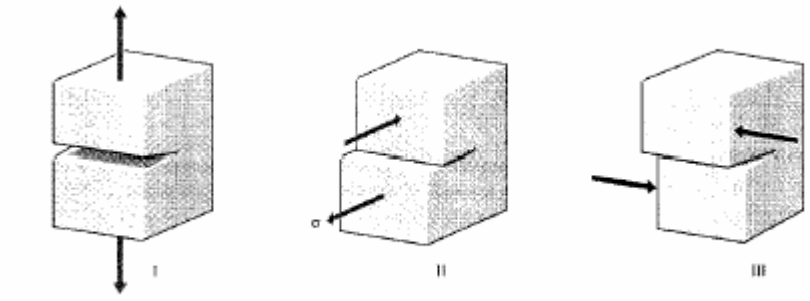

Figure 5 Fracture modes

There are three modes of cracks[3], termed mode I, II, and III as illustrated in figure 5. Mode I crack is a normal-opening mode and is the one common, while modes II and III

are shear sliding modes, the semi-inverse method developed by Westergaard shows the opening-mode stresses to be

$$\sigma_x = \frac{K_I}{\sqrt{2\pi r}} \cos\frac{\theta}{2}\left(1 - \sin\frac{\theta}{2}\sin\frac{3\theta}{2}\right) + \dots$$

$$\sigma_y = \frac{K_I}{\sqrt{2\pi r}} \cos\frac{\theta}{2}\left(1 + \sin\frac{\theta}{2}\sin\frac{3\theta}{2}\right) + \dots \quad . \qquad (1)$$

$$\tau_{xy} = \frac{K_I}{\sqrt{2\pi r}} \cos\frac{\theta}{2}\cos\frac{3\theta}{2}\sin\frac{\theta}{2}\dots$$

For distances close to the crack tip ($r \leq 0.1a$), the second and higher order terms indicated by dots may be neglected. Here a is crack length and r is crack tip radius. At large distances from the crack tip, these relations cease to apply and the stresses approach their far-field values that would obtain were the crack not present. The K_I in Equations 1 is a very important parameter known as the stress intensity factor. The I subscript is used to denote the crack opening mode, but similar relations apply in modes II and III. The equations show three factors that taken together depict the stress state near the crack tip: the denominator factor $(2\pi r)^{-1/2}$ shows the singular nature of the stress distribution; σ approaches infinity as the crack tip is approached, with a $r^{-1/2}$ dependency. The K_I factor gives the overall intensity of the stress distribution, hence it is called stress intensity factor. The K depends upon the applied stress, the size and the placement of the crack, as well as the geometry of the specimen. The general form stress intensity factor is:

K = f (load, crack length, geometry)

For mode I behaviour stress intensity factor is:

$$K = \left(\frac{EG}{1-(\alpha\nu)^2}\right)^{1/2} \qquad (2)$$

Where E is the young's modulus and ν is the Poisson's ratio. The value of α ranges from 0 for plane stress and 1 for plane strain

In more general form the above equation can be written as

$$G = \frac{B}{E}\left(K_I^2 + K_{II}^2\right) + \left(\frac{1+\nu}{E}\right)K_{III}^2 \qquad (3)$$

Where B = 1 for plane stress and $1-\nu^2$ for plane strain.

Another important relationship for stress intensity factor in linear elastic analysis is based on the Westergaard equations which links the stress intensity factors to the CTOD (crack tip opening displacement) as

$$K_I = \frac{EV_i}{4B}\sqrt{\frac{2\pi}{r}}, \quad K_{II} = \frac{EV_{ii}}{4B}\sqrt{\frac{2\pi}{r}}, \quad K_{III} = \frac{E}{2(1+\nu)}V_{iii}\sqrt{\frac{\pi}{2r}} \qquad (4)$$

Where Vi, Vii, and Viii are the relative opening displacements at a radius r from the crack front for an orthogonal system aligned with mode I, II, and III directions. This approach is widely used by the practitioners of both FEM and BEM. But the drawback to this method is that it requires a state of stress assumption.

J-integral is another parameter commonly used in crack propagation analysis. The J – integral concept was first described by Rice in the late 1960s. It is an energy based concept that is widely used in fracture mechanics. It is path independent line integral when contours are taken around crack tip. For linear elastic materials the value of J is equal to the energy release rate associated with crack advance.

For isotropic linear elastic materials,

$$J = G = \left(\frac{1-\nu^2}{E}\right) K^2 \qquad \text{For plane strain and} \qquad (5)$$

$$J = G = \frac{K^2}{E} \qquad \text{For plane stress} \qquad (6)$$

The J – integral and stress intensity factors are closely related to the energy release rate associated with infinitesimal crack growth in an isotropic linear elastic materials. Energy release rate G, represents the amount of work associated with a crack opening or closure. A number of criteria have been developed to specify the direction. They include the maximum energy release rate, maximum tangential stress, and the normal to maximum principal stress. In the context numerical calculations of energy release rate and the stress intensity factor.

$$\theta = \tan^{-1}\left(\frac{K_{II}}{K_I}\right) \qquad (7)$$

For elastic plastic fracture mechanics the crack tip opening displacement (CTOD) is a measurement of the crack opening displacement at the crack tip. The relationship between J and CTOD (δ) is given by the equation:

$J = m\ \sigma_{ys}\ \delta$

where m varies between 1.15 and 2.95. For such elastic plastic cases the difficulty of using this method is choosing a valid value of m.

4. Numerical issues in evaluating crack propagation

There are two major numerical approaches available to fracture parameters

1 Boundary element method
2 Finite element method

The finite element method is the most popular approach for tackling the fracture mechanics problems. This requires the discretization of the complete structure. The main advantages of the leading finite element codes is the flexibility that they provide in terms of non-linearity and overall analysis capability. There are many commercial packages available like ABAQUS, ZENCRACK, for use in fracture mechanics applications.

Crack growth integration scheme

Once a method is selected to calculate fracture parameters, the next step is crack growth calculation. For a given material the crack growth rate, da/dN, is a complex function of many variables including stress intensity range (ΔK = Kmax – Kmin), stress ratio, (R = Kmin/ Kmax), temperature and frequency of the applied cyclic load. Crack growth is generally calculated using one of the parameters K or G. For fatigue crack growth the simplest equation which relates the loading and material due to crack growth and fatigue cycles is the Paris equation of form:

$$\frac{da}{dN} = C(\Delta K)^{m} \tag{8}$$

here a = crack size
N = number of fatigue cycles.
C, m = material constants
ΔK = stress intensity factor range.

Also from Walker equations:

$$\frac{da}{dN} = C_o(\Delta K_o)^n, \quad \Delta K = \Delta K_o(1-R)^{(1-m)}$$

gives

$$\frac{da}{dN} = C_o\left[\Delta K(1-R)^{(m-1)}\right]^n \tag{9}$$

where subscripts 0 refers to the values at R = 0.

In order to complete the crack growth prediction, it is necessary to integrate using the fracture mechanics parameters from finite element analysis along with the crack growth data and load history.

In many cases the effect of static load needs to be combined with cyclic external load. The ability to include static load or residual stress effect is an important feature of the crack growth integration scheme. The consequence of the static load is to modify the instantaneous stress ratio. For cyclic load that gives a K range between the $K_{cyclicmax}$ and $K_{cyclicmin}$ at a node for which the static load gives K_{static} then:

$$R_{effective} = \frac{K_{cyclic\,\min} + K_{static}}{K_{cyclic\,\max} + K_{static}} \tag{10}$$

The data required for crack growth analysis

1) Cyclic crack growth data, da/dN Vs ΔK
    - Simple forms e.g. Paris (equation 8), Walker (equation 9)
    - Tabular data as a function of R, temperature
2) Time dependent crack growth data da/dt Vs K
3) Threshold and Fracture derived from da/dN curve.

The fatigue crack growth can occur under constant or variable amplitude cyclic loading. In order to use this type time series loading for fatigue crack growth calculation, it must be first converted into a cycle counted spectrum. The most commonly used technique as rainflow counting technique for this. The result of this count is a load spectrum in which each cycle has a specified minimum and maximum load level. The stress ratio, R for the cycle is the ratio of minimum to maximum loads.

Rainflow cycle counting

Rainflow cycle counting derives its name from an analogy to the flow of rain water off multiple sloping roofs. Strain history is oriented with time axis vertical and strain axis horizontal. Strain ranges (cycles) is counted when a stream of water meets an immediate lower roof. After a cycle is counted the peaks are edited from the history. This method cycles are counted on the basis of closed hysteresis loops in the stress-strain history.

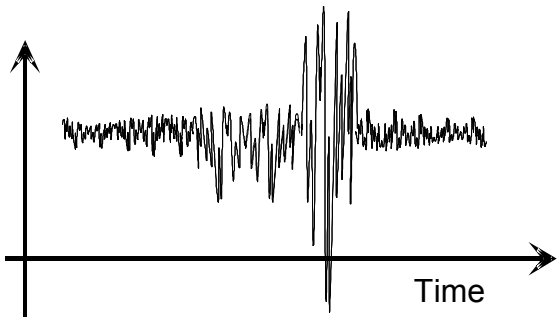

Figure 6 Variable amplitude loading.

The Rainflow cycle counting converts the complicated load function (random loading) to equivalent load cycles. Load X(t) gives amplitudes S1,S2,S3..Sn. This method is used to identify stress reversals and Miner's rule is used to perform the damage summation. The following figure 7 shows the rain flow counting method[4].

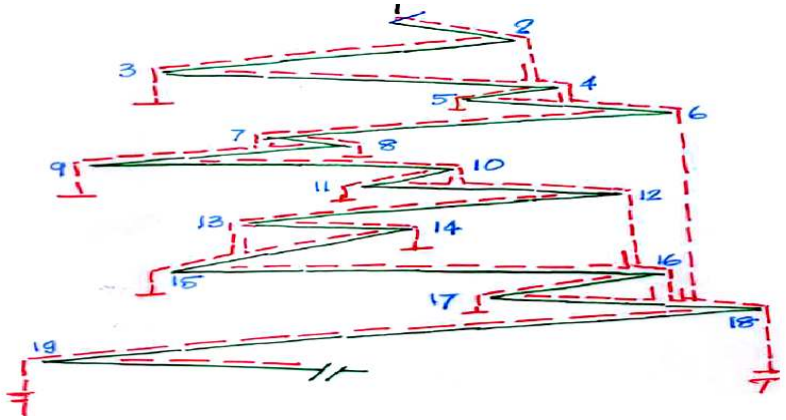

Figure 7. Rainflow counting

The basic load-time data and the counted cyclic load data are the fundamental load history inputs for time dependent and fatigue crack growth calculations respectively.

5. Modeling crack growth in ABAQUS

ABAQUS includes modeling and post-processing capabilities for fracture mechanics analyses. These features provide interactive access to the contour integral fracture mechanics technology in ABAQUS/Standard. With these tools models can be created to estimate *J*-integrals, stress intensity factors, and crack propagation directions**.** Here a example of a standardized compact tension specimen is modeled, and ***J***-integral results are compared with those generated from applicable American Society for Testing and Materials (ASTM) standards and from a laboratory testing method. It is shown that ABAQUS results are in very close conformance with the experimental results.

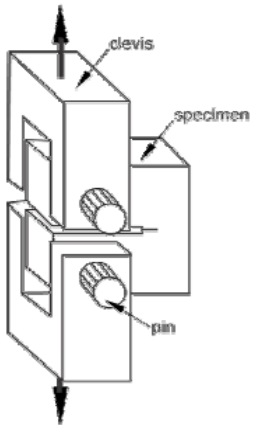

Figure 8. Apparatus for testing compact tension specimen[5,6]

The compact tension (CT) specimen has been standardized by the ASTM for use in the experimental determination of the fracture toughness of metallic materials. A schematic diagram of a CT specimen testing apparatus is shown in above figure 8. A clevis and pin arrangement is used to hold the specimen. The pre-cracked specimen is loaded at a controlled rate, and the resulting load-displacement data are recorded. Analysis of the experimental data allows the material fracture toughness to be determined in terms of the stress intensity factor K or the ***J***-integral. ***J***-integral values are computed and compared to those calculated with standard analytical methods.

6. Finite Element Analysis

The dimensions of the specimen under consideration are shown in figure 9. The initial crack length (not shown) is 5 mm

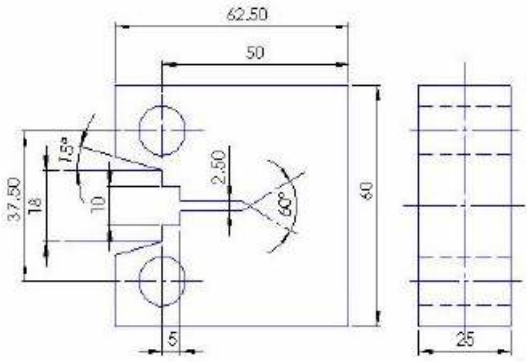

Figure 9. Compact tension Specimen (all dimensions are in mm)

The elastic modulus of the specimen material is 213 GPa, and Poisson's ratio is 0.3. The yield stress is approximately 715 MPa, and the true stress versus logarithmic strain curve for this material is plotted as in figure 10.

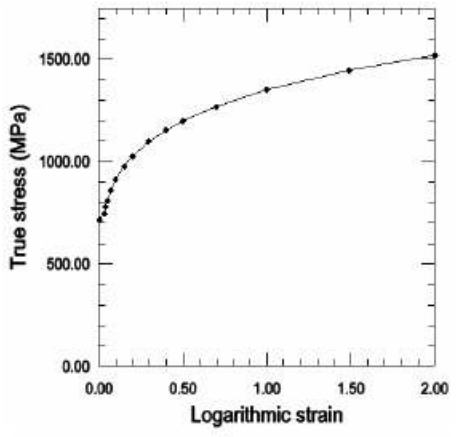

Figure 10. True stress-logarithmic strain curve for specimen material.

A two-dimensional plane-strain model is analyzed in ABAQUS. The loading pins are modeled as rigid bodies. The specimen is loaded by applying a displacement to the pins in the vertical direction; all other motions of the pin are restrained. Surface to surface contact with a finite-sliding formulation is defined between the pins and the specimen. Two analysis steps are used. In the first step contact is established between the pins and the specimen by applying a small displacement (1×10^{-5}mm) in the vertical direction. In the second step controlled displacement loading of the pins is applied.

Modeling in ABAQUS

The partitioned geometry of the model is shown in figure 11. The load line displacement, which will be needed for post-processing purposes, is evaluated at the points marked by yellow dots.

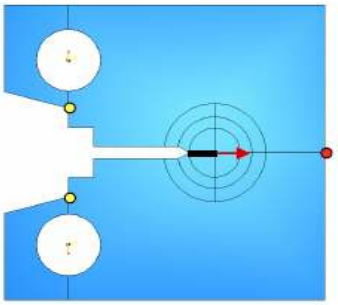

Figure 11. Partitioned two-dimensional compact tension specimen

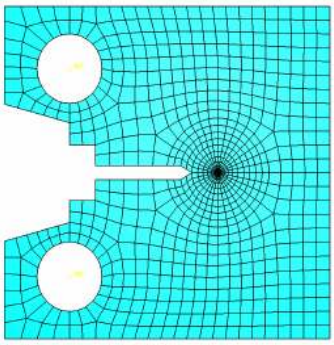

Figure 12. A focused mesh with elements having collapsed edges around the crack tip

The circular partitioned areas are meshed using the "swept meshing" technique; this method allows the mesh to be regular and focused. The inclusion of the seam and singularity definition causes ABAQUS to create automatically collapsed elements with correct connectivity definitions. The remaining portion of the model is free meshed using the "medial axis" meshing algorithm. The edge-based tools for specifying mesh seeding facilitate the development of a focused mesh around the crack tip. The results obtained from ABAQUS for the ***J***-integral are compared with the results computed by ASTM standard methods and with the laboratory testing method used in reference[6].

Table 1 Comparison of J –integral values

Load line displacement (mm)	*J*-integral (N/mm)		
	ABAQUS (5^{th} contour)	ASTM (E1737-96)	Anderson (Ref. 1)
0	0	0	0
0.0797	6.33	6.19	6.296
0.159	24.99	23.87	24.828
0.239	55.03	56.53	54.696
0.319	95.24	98.88	94.69
0.399	144.03	148.19	143.194
0.479	198.78	203.19	197.58
0.559	255.69	259.01	254.58
0.639	313.3	312.7	312.43
0.719	371.45	371.86	370.956
0.8	430.05	425.78	430.05

As seen in Table 1, the results obtained from ABAQUS are in very close conformance with the results computed using ASTM standards and the method in Reference[6].

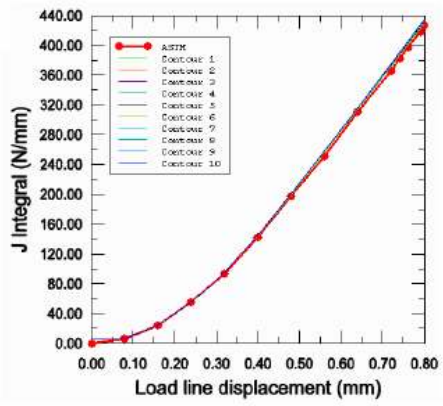

Figure13. J-integral results obtained for 10 contours using small-strain analysis

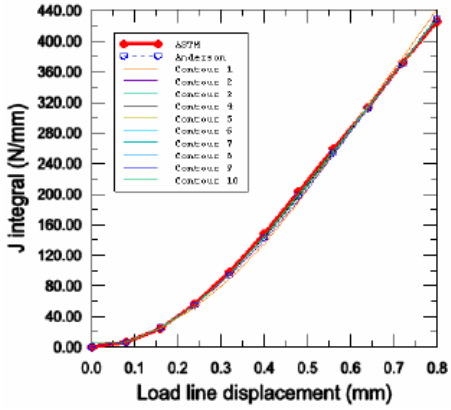

Figure 14. J-integral results obtained for 10 contours using finite-strain analysis

In figure 13 the ***J***-integral values for all analysis methods are plotted. Usually the ***J***-integral for the first contour is ignored because of numerical inaccuracies in the stresses and strains at the crack tip. The effect of the inaccuracy is less pronounced in small-strain problems than in finite-strain problems. A second set of analyses was conducted in which finite strains were considered and the crack front region was selected to be larger than the plastic zone around the crack tip. The ABAQUS results are compared only with the ASTM calculation, since these depend only on the load-displacement behavior of the specimen and not the strain magnitudes at the crack tip. The results from the second analysis set are shown in figure 14. It is clear that the ABAQUS results are in very close

conformance with the ASTM standard results. The inclusion of finite-strain effects only changes the results slightly for this analysis because the nonlinearity in the analysis is highly localized at the crack tip and does not affect the global behavior.

Examples of Crack Growth: Using ZENCRACK

Compressor disc spin test

A spin disc crack, reported in literature by Zuang[7] has been undertaken to demonstrate 3D crack growth modeling using FEM. Figure 15 shows the cracked compressor disc details of which are given by Zuang[7]. An initially quarter circular corner crack grows from bolt hole in the disc and breaks through the full crack and growth continues until the disc fails.

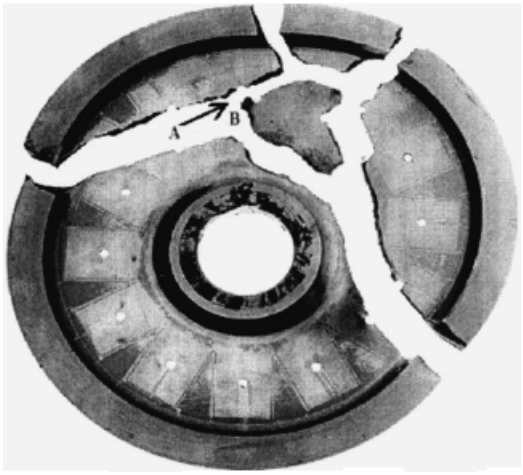

Figure 15 Failure in Ti alloy compressor disk due to defect growing from hole A to B

The un-cracked model used for the analysis consists of 216 solid 20 noded-brick elements of ABAQUS element type C3D20. The geometry of the model was limited to a segment of the compressor disc between the center lines of the two adjacent bolt holes (figure 15). The bolt holes are 4.76 mm diameter and the disc is 3mm thick at the bolt-holes (for other dimensions refer[7]). The material is Ti-8Al-1Mo-1V titanium alloy with $E = 126000$ MPA, $\nu = 0.33$, $\rho = 4373$ Kg/m^3 and $\sigma_y = 922$ MPa. The entire model is subjected to a centrifugal load corresponding to a constant amplitude load cycle for rotation of 37000 rpm to 8000 rpm about the three axes, where the center of rotation is defined as the center of the whole compressor disc.

Figure 18[8] shows the (linear elastic) Von Mises stress distribution for the model at a rotational speed of 370000 rpm. The background stress around the bolt-hole is found to be approximately 650 MPa, and increase by a factor of 2 to 1300 MPa. at the edge of the bolt-hole where the stress state is approximately equi-biaxial. These findings agree precisely with those give in Zhuang[7]. In an elastic-plastic analysis, the material surroundings the bolt-hole will clearly undergo plastic deformation at the peak rotation speed of 37000 rpm. Zhuang[7] uses a weight function and superposition technique to

generate a distribution of non-dimensional stress intensity factor, f, against a crack size for a crack emanating from a hole under bi-axial loading.

Spin test crack growth data

Zhuang[7] presents the crack growth data in the following two forms:

1. da/dN Vs ΔK data at stress ratios of R = 0.0, 0.25, 0.43, 0.676 and 0.85.
2. da/dN Vs ΔK_{eff} for the corner and through crack phases obtained from raw data at four stress ratios.

$$\frac{da}{dN} = C(\Delta K_{eff})^{m}$$

where C = 3.16 x 10^{-10} and m = 2.86 for corner crack growth
C = 2.6 x 10^{-10} and m = 3.14 for through crack growth

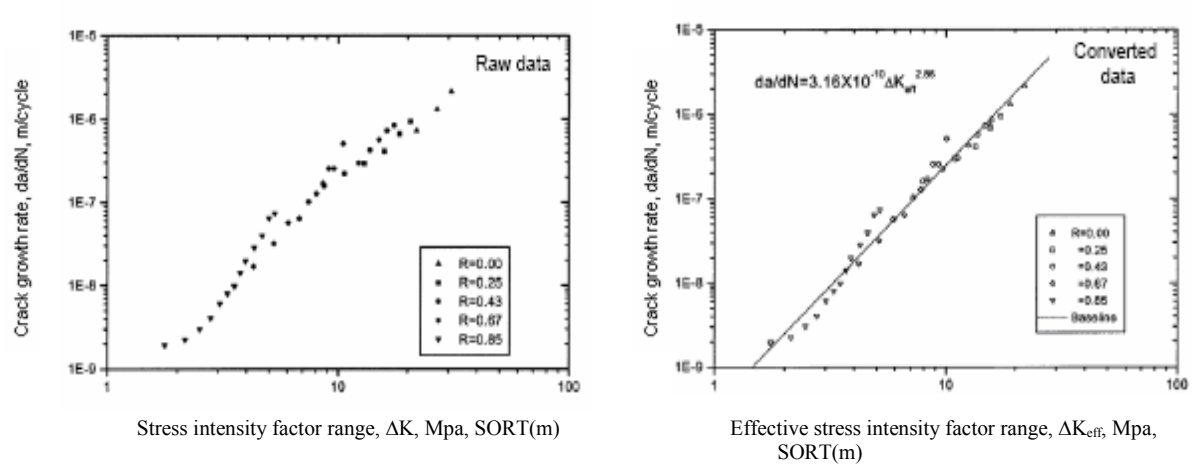

Stress intensity factor range, ΔK, Mpa, SORT(m)

Effective stress intensity factor range, ΔK_{eff}, Mpa, SORT(m)

Figure 16 Graph da/dN Vs ΔK and da/adN Vs ΔK_{eff}

The effective data is obtained by using the crack closure model presented by Newman[9]. to account for plasticity induced crack closure, as defined in equation 11.

$$\Delta K_{eff} = \left(\frac{\sigma_{max} - \sigma_o}{\sigma_{max} - \sigma_{min}} \right) \Delta K \qquad (11)$$

where σ_o = crack opening stress
σ_{max} = 650 MPA (at 37000rpm)
σ_{min} = 30 MPA (at 8000rpm)

The comparison of the da/dN Vs ΔK and da/dN Vs ΔK_{eff} given in figure 16 of Zhuang[7] revealed variation in the σ_o depending on the test data stress ratio, R. Values ranged from around 200 MPa at R = 0, to approximately 50 MPa for R = 0.85. Methods based on the crack closure model described in Newman[9] were used to obtain an approximate value of the crack opening stress for the spin-test stress ratio of R = 0.04615. For an assumed geometric constraint factor of C = 1.12 (based on a through crack in a plate), σ_o was found to be approximately equal to 81.6 MPa. An alternative method of approximating the opening stress is obtained by breaking down an elastic-plastic ABAQUS analysis in to a number of load steps to identify the load level at which the crack ligament is fully inside. One load cycle was slit into 2000 increments to reveal, for a range of crack sizes, an average opening stress of 325 MPa. In ZENCRACK[8] the Paris relation must be defined in terms of ΔK rather than $\Delta K_{eff.}$ For the corner crack phase, the following values for C and m can be therefore considered:

$$\frac{da}{dN} = C(\Delta K_{eff})^m$$

$C = 1.26413 \times 10^{-11}$ and m = 2.86 back calculated from ΔK_{eff} with $\sigma_o = 81.6$ MPa (12)
$C = 2.55525 \times 10^{-12}$ and m = 2.86 back calculated from ΔK_{eff} with $\sigma_o = 325$ MPa (13)
$C = 1.08227 \times 10^{-12}$ and m = 3.11527 straight line fit to raw data at R = 0 (14)
$C = 1.58039 \times 10^{-12}$ and m = 3.1487 straight line fit to raw data at R = 0.25 (15)

It is noted that the "raw" test data corresponds to a load range much lower than that involved in the spin test analyses -the mean load of 173MPa compares to a mean of 325MPa for the spin test. Further, the R = 0 and 0.25 curves are defined by only three points, the upper point falling at the lower end of the ΔK range for the spin test. The straight line approximations from the three points have been assumed to apply to higher ΔK values than provided by the test data.

The initial quarter circular comer crack has radius 0.39mm. This has been analysed under the crack growth laws of Equation 12 to Equation 15. The linear elastic finite element analyses are carried out at a load level of 37000rpm and the stress ratio of 0.046 is applied to give a range of K. In many cases of crack growth prediction, particularly under constant amplitude loading, the effects of local crack tip plasticity are ignored and LFEM is applied. In this analysis there is a significant amount of plasticity at the bolt hole due to the high load level in the structure. If the crack is included and elastic-plastic analysis is carried out, the plastic strain distribution will be affected by the presence of crack. To include a representative plastic strain distribution at the bolt hole, the following procedure is used:

1) Include the crack and tie the crack faces together to effectively produce an uncracked model.
2) Load to 37000rpm to develop plastic strains around the bolt hole.
3) Release the crack face tying constraint to allow the crack to open up.

It was found that with this method the compressive stresses at the low load level caused the crack faces to close. The closure effect is greatest along the bolt-hole bore edge. This is illustrated by contact pressure of the crack face shown in figure 19.

To analyze the crack growth with plastic strains introduced as described above requires a definition of suitable range stress intensities. Due to the closure effects at the low stress level, the range is taken from 0 to Kmax. When the effect was analysed under these conditions crack growth was hindered by “burrowing” of the crack front, resulting in premature halting of the analysis. The example of burrowing crack profiles is shown in figure19. The final crack position for the corner crack phase was used to estimate a starter slanting crack for through crack phase. Results of the analysis using linear elastic and elastic plastic finite element analysis are shown in figure 21.

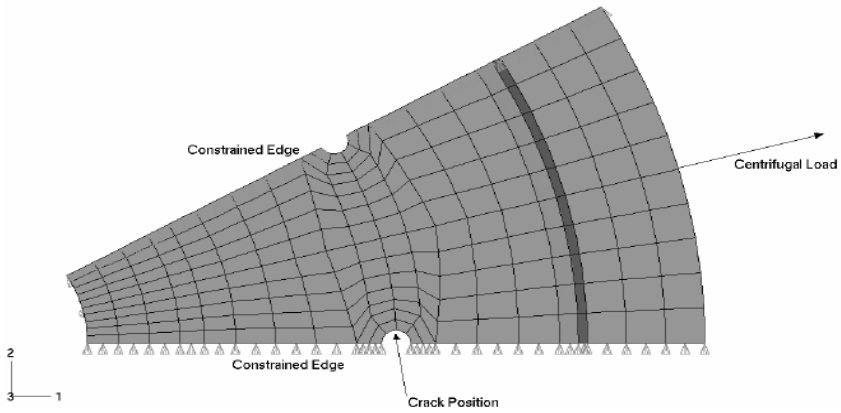

Figure 17. Un-cracked mesh model of spin disc.

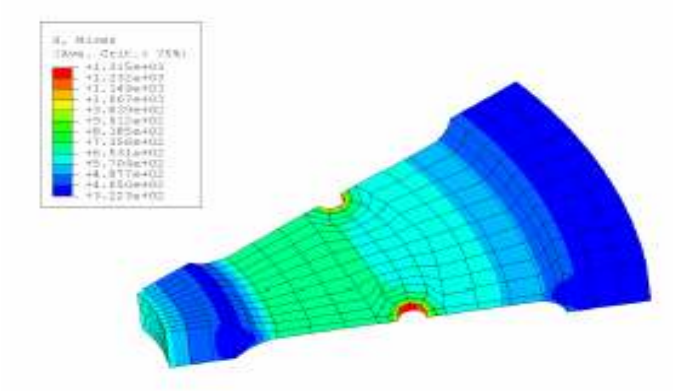

Figure 18. Von Mises stress plot for un-cracked disc

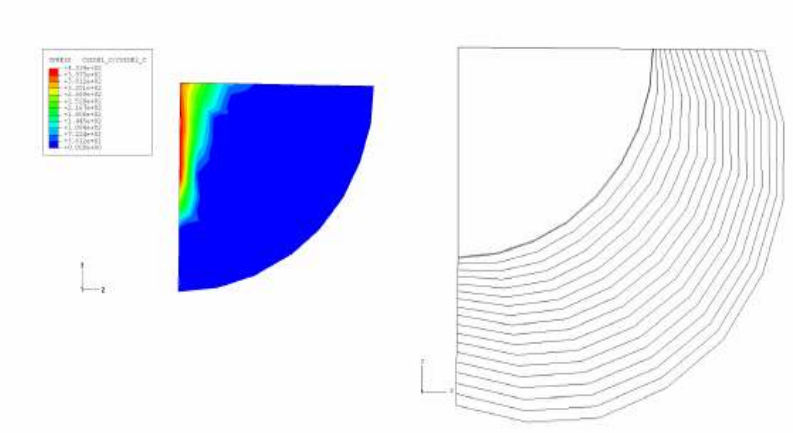

Figure 19. Contact pressure and crack growth rings

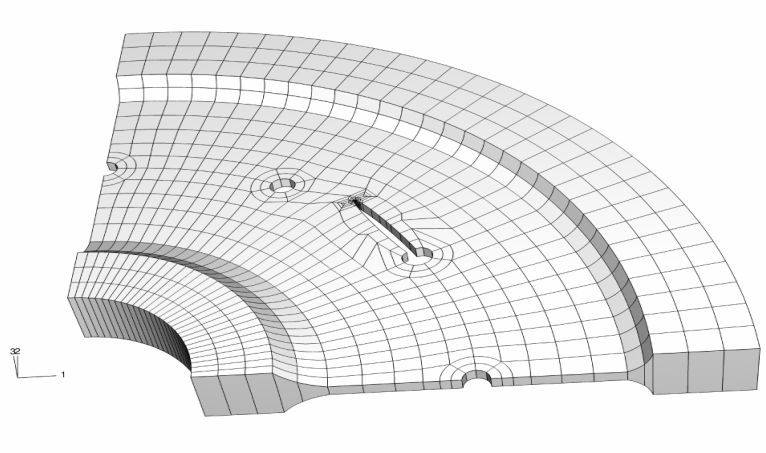

Figure 20. Crack propagation in spin disc from bolt hole to bolt hole.

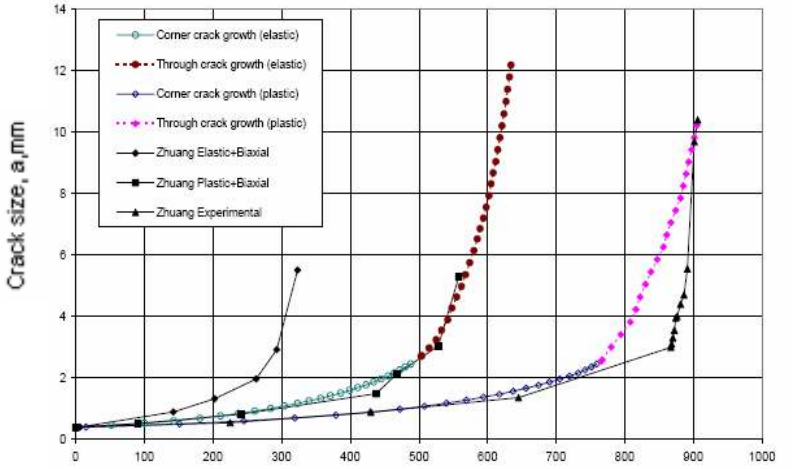

Figure 21. Final predictions-large crack growth corner and through crack phases

7. Conclusion:

A method was demonstrated for allowing the crack prediction in 3D models. This new method allows considerable improvement on crack growth prediction capabilities that were previously available. The method described in this paper provides powerful capabilities to ABAQUS and ZENCRACK. Finite element codes are able to accurately simulate complex real world problems. FEM models can be validated with experimental results so that it can be effectively used for different factors to be explored without a need for any expensive experimental testing.

8. References:

1. David L McDowell, "Models for small fatigue crack growth", Robust Engineering Models for Integrated Prognostics.
2. R. Sunder, "Incorporating service conditions in fatigue design and testing", National seminar on Fatigue, Reliability and performance considerations in design" 14th -15th July, IISC, Bangalore.
3. David Roylance, "Introduction to Fracture Mechanics", Department of Materials Science and Engineering, Massachusetts Institute of Technology, Cambridge, MA 02139, June 14, 2001.
4. K N Raju, "Damage tolerance allowables for design of air frames of transport aircraft", National seminar on Fatigue, Reliability and performance considerations in design" 14th -15th July, IISC, Bangalore.
5. Anderson T.L. "Fracture Mechanics: Fundamentals and Applications", CRC Press, 1991.
6. ASTM Standards, "Test Method for J-integral characterization of fracture toughness", ASTM E1737-96", American Society for Testing and Materials, Philadelphia, 1997.
7. W Z Zhuang, "Prediction of crack growth from bolt holes in a disc", International Journal Fatigue, 22(2000) 241-250.
8. R. Chandwani, C M Timbrell, M Wiehahn, "An FE Simulation Tool for Fracture Mechanics", National seminar on Fatigue, Reliability and performance considerations in design" 14th -15th July, IISC, Bangalore.
9. Newman J.C.(1981), "In: Methods and Models for predicting Fatigue crack Growth Under Random Loading", pp. -53-84 Chang, J.B. and Hudson, C.M.(Eds), ASTM STP 748.
10. G. Cook, Timbrell, Browning, "The application of 3D Finite Element Analysis to engine life prediction", AeroMat 2001- 12th Advanced Aerospace Materials and Processes Conference & Exhibition, Long beach, CA, USA.
11. Ben Browninig, Gerry Cook, Chris Timbrell, "Prediction of large scale crack growth in 3D finite element models" Zentech International Ltd.
12. M. R Roy, J D G Sumpter, C M Timbrell and M Wiehahn "Stress intensity factors for cracked plates under out-of-plane bending" , Zentech International Ltd.
13. Newman, J.C. (1976), In: Mechanics of Fatigue Crack Growth, pp. 281-301, ASTM STP 590.
14. Mary Todd, "Finite Element Study of Stress Ahead of Crack Tip for Fatigue Crack Growth Prediction", Western Michigan University, Technical report Number MAE-04-07, July 2004.